Article

Assessing the Impact of Climate Change on the Biodeterioration Risk in Historical Buildings of the Mediterranean Area: The State Archives of Palermo

Elena Verticchio [1], Francesca Frasca [2,3], Donatella Matè [4,†], Federico Maria Giammusso [5], Matilde Sani [2], Maria Letizia Sebastiani [6,†], Maria Carla Sclocchi [6,†] and Anna Maria Siani [2,3,*]

1   Institute of Heritage Science, National Research Council, Via Salaria km 29,300, 00015 Montelibretti, Italy; elena.verticchio@ispc.cnr.it
2   Department of Physics, Sapienza University of Rome, P. Le Aldo Moro, 00185 Rome, Italy; f.frasca@uniroma1.it (F.F.)
3   Research Center for Applied Sciences to the Safeguard of Environment and Cultural Heritage, Sapienza University of Rome, P. Le Aldo Moro, 00185 Rome, Italy
4   Istituto Centrale per la Patologia degli Archivi e del Libro, Ministero della Cultura, Via Milano 76, 00184 Rome, Italy
5   Archival Superintendence of Sicily, State Archives of Palermo, Ministero della Cultura, Via Vittorio Emanuele 31, 90133 Palermo, Italy
6   Institute for Biological Systems, National Research Council, Via Salaria km 29,300, 00015 Montelibretti, Italy
*   Correspondence: annamaria.siani@uniroma1.it
†   Retired.

Abstract: The growing sensitivity towards environmental sustainability, particularly in the light of climate change, requires a reflection on the role that historical buildings can play in heritage conservation. This research proposed an interdisciplinary approach combining climate and biological expertise to evaluate the biodeterioration risk associated with different IPCC outdoor climate scenarios. Conduction heat transfer functions and dose–response functions were used to model the indoor climate of a historical building and the related climate-induced risk of mould and pest proliferation. The approach was applied to a case study in the Mediterranean area, i.e., the State Archives of Palermo (Italy) housed in a 15th-century convent. In 2018, a survey conducted by ICPAL-MiC experts warned about past infestations and risks deriving from climate conditions. An environmental monitoring campaign conducted in 2021 allowed for the characterisation of the buffering effect in a historical building in response to the outdoor climate and the simulation of future indoor climate. Since indoor temperature and mixing ratio are expected to raise in future scenarios, it was found that there is an increased risk of insects' proliferation, combined with a decreased risk of spore germination and mould growth. Such evidence-based evaluation allows for the design of tailored preventive conservation measures to enhance the durability of both the archival collections and the building.

Keywords: climate change scenarios; historical building simulation; preventive conservation; biodeterioration risk assessment; historical archive; Intergovernmental Panel on Climate Change

1. Introduction

Over the past decades, scientific research has made considerable progress in the knowledge of materials' vulnerability to environmental conditions. In parallel, the awareness of the need for preventive conservation (PC) has been increasing, as it involves "all measures and actions aimed at avoiding and minimising future deterioration or loss" [1]. The risk management approach in PC is based on the identification, analysis, and prioritisation of the risks for the heritage assets [2]. Interdisciplinary studies provide the best possible grounds for comprehensively diagnosing and mitigating the different kinds of deterioration under existing and climate-change conditions. Indeed, to understand the multiple

aspects responsible for deterioration and provide a thorough assessment of the risks, it is necessary to involve a variety of expertise in different and complementary disciplines (biology, chemistry, physics, material science, conservation, etc.).

Climate studies can significantly contribute to PC by reducing the risk of climate-induced decay of materials. The materials' deterioration due to specific climate exposure can be modelled using dose–response functions (DRFs) [3], i.e., equations expressing the relationship between the accumulated dose of a hazard (e.g., environmental factors) and measurable changes in a material (e.g., deformation). DRFs can be used to assess the mechanical, chemical, and biological risks for various materials constituting heritage objects such as stone, paper, and wood. Several authors have focussed on developing specific DRFs aimed to assess the impact of outdoor climate conditions on the deterioration of various heritage settings [4,5]. Similar approaches have been followed for indoor applications [6], highlighting the advantage of using numerical tools to derive the influence of an outdoor forcing on the indoor climate conditions [7–9].

The principal biodeteriogens affecting heritage conservation are moulds [10], insects [11], rodents, and less frequently birds and bats. Among the five stages followed to control the risks (avoid—block—detect—respond—recover) [2], detecting the presence of biodeteriogens and assessing the possible impact of biodeterioration are crucial to planning effective and timely PC strategies. Integrated pest management (IPM) proposes a long-term holistic strategy to minimise biologically induced risks on cultural heritage [12] by possibly reducing the application of biocides while establishing environmental conditions less favourable for pests' proliferation [12–14]. Although active climate control can contribute to limiting biodeterioration, the ever-growing demand for sustainability also in the PC field compels us to avoid (or at least reduce) the use of energy-demanding and expensive mechanical ventilation systems especially in the case of low-energy-efficient buildings such as the historical buildings [15].

Climate change poses new serious threats to the durability of climate-vulnerable objects exposed to outdoor conditions [4,16] as well as objects housed indoors [17,18]. During the latest Conference of the Parties (COP27) of the United Nations Framework Convention on Climate Change (UNFCCC) in 2022, the critical linkages between cultural heritage and climate change have been finally acknowledged [19,20]. Indeed, the increasing occurrence of extreme events due to ongoing global warming, as already projected by the Intergovernmental Panel on Climate Change (IPCC) in the Fifth and then reconfirmed in the Sixth Assessment Reports [21,22], may further reduce the durability of climate-vulnerable objects [5,23,24]. Moreover, as higher temperatures can enhance biodeterioration risks being responsible for the migration and adaptation of new species of biodeteriogens [25], global warming can increase the deterioration risks related to biodeteriogens [17,25].

Historical buildings, thanks to their heavyweight structures (e.g., massive masonry) conceived to deal passively with the specific local climate [26], can attenuate the effect of outdoor climate fluctuations on indoor conditions. For this reason, when they are unconditioned (i.e., not equipped with systems for climate control such as radiators and fan coils), the study of their natural historical indoor climate [6] and their free-floating response to the outdoor fluctuations can support the design of passive environmental improvement solutions [27]. Since the PC strategies should be designed based on the indoor climate, building models can be effectively exploited to explore the indoor climate conditions deriving from building features [28] and outdoor climate [9,29]. The modelling approach was extensively adopted within the European projects Noah's Ark (2004–2007) [30] and Climate for Culture (2009–2014) [7] to derive the deterioration risks for cultural heritage related to outdoor and indoor climate scenarios. Nevertheless, a recently published review reported that there is still a lack of studies directly involving climate scenarios for an evidence-based evaluation of its impact [31]. Being the indoor climate in unconditioned historical buildings mostly influenced by the outdoor one, transfer functions (TFs) can be used to reconstruct the indoor climate conditions starting from the assessment of the building response.

This paper presents an interdisciplinary study aimed to evaluate climate-induced biological risks in different IPCC climate scenarios. The approach was applied to the State Archives of Palermo (Italy), housed in a 15th-century convent, where a survey conducted in 2018 warned about past infestations, and a climate monitoring campaign started in 2021 to assess risks deriving from the climate conditions.

Section 2 deals with the description of this case study, the climate monitoring campaign started in 2021, and the characterisation of the response of the historical building based on the climate observations collected over a year. The methods used for simulating future indoor climate scenarios and assessing the related biodegradation risks are also described here. Sections 3 and 4 are devoted to the presentation and discussion of the results. Section 5 outlines the main conclusions of the work.

2. Materials and Methods

2.1. Case Study, Biological Technical Survey, and Climate Monitoring

The State Archives of Palermo (Lat. 38.12° N, Lon. 13.37° E, 8 m a.m.s.l, Köppen-Geiger climate class *Csa*, i.e., temperate climate, with dry and hot summer [32]), was instituted in 1843 as "Grand Archive" by the Sicilian Parliament, which established a General Archive to collect the documents of the Kingdom of Sicily and, later on, the Kingdom of Naples. Since 1975, the State Archives of Palermo has been working as a peripheral organ of the *Ministero per i Beni Culturali e Ambientali* (today *Ministero della Cultura*, MiC).

The Gancia headquarters is in the former Franciscan convent of *Santa Maria degli Angeli*, also known as *Santa Maria della Gancia*, or simply *La Gancia*, which is also adjacent to the church of the same name dating back to the late 15th century (Figure 1a,b). The monumental complex is characterised by heavyweight sandstone masonry (on average 1.8 m thick) with historical metal-framed single-pane unshaded windows.
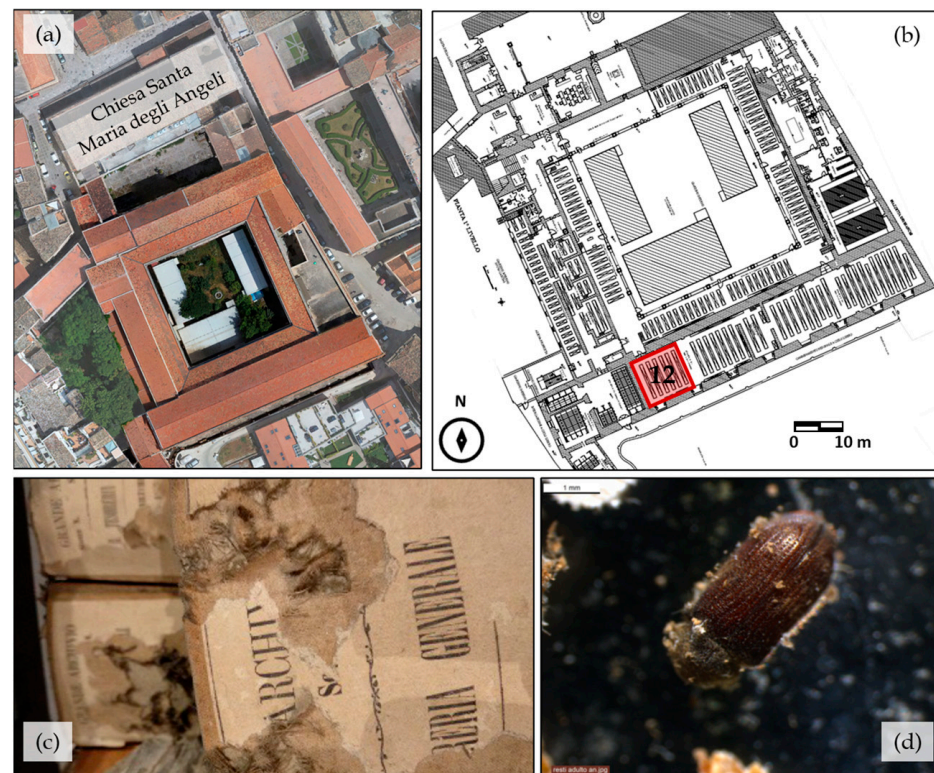

Figure 1. (**a**,**b**) External view (Google Earth source) and plan of the first floor of La Gangia housing the State Archives of Palermo, Room 12 is located in the red area; (**c**,**d**) pictures taken during the technical survey conducted by the experts from *Istituto Centrale per la Patologia degli Archivi e del Libro* (namely ICPAL-MiC).

Past infestations of biodeteriogens were documented in 1952 [33]. In November 2018, a technical survey was conducted by the experts from *Istituto Centrale per la Patologia degli Archivi e del Libro* (namely ICPAL-MiC) in selected rooms of the Archives. During the inspection, damages on archival folders caused by rodents (Figure 1c) were reported, and previous signs of entomological attacks (e.g., exuviae of coleopters) on the leather covers of the archival folders were sampled (Figure 1d). The water content in the folders, measured using a portable moisture analyser, resulted to be too low for the preservation of paper documents (<6%). Although no evident signs of active biodeterioration by microorganisms nor of entomological attacks were reported, it was advised to reduce direct solar radiation entering the room and to install a densely meshed mosquito net on external windows to prevent the access of small Arthropoda (e.g., insects and arachnids that could become a nutritional source for other organisms) while maintaining ventilation in the room.

A climate monitoring campaign was implemented in 2021 to assess current climate conditions in a room of the Archives (Room 12) and to evaluate possible risks also related to possible climate-change conditions. One thermo-hygrometer (hereinafter called RHT), manufactured by Stego (model CSS 014), was installed to measure temperature (T) and relative humidity (RH) at local time. Room 12 (red area in Figure 1b) is located on the ground floor of *La Gancia* monumental complex, with one south-facing single-pane French door, and is not provided with any climate control system (i.e., has unconditioned free-floating conditions). The uncertainties of the Pt100 resistance thermometer for T and thin-film capacitive sensor for RH equal to $\pm 0.3\,^{\circ}C$ and $\pm 3.0\%$ (from 20 to 80% at 5–60 °C), respectively, were in line with the current European Standards on the instruments recommended in cultural heritage conservation [34,35]. The monitoring started on 1 May 2021, with a sampling frequency set to 30 min, and it is still ongoing.

Outdoor T and RH data used in this analysis were gathered from the weather station of *Osservatorio Astronomico di Palermo "G.S. Vaiana"* (Lat. 38.11° N, Lon. 13.35° E, 75 m a.m.s.l), at 1.5 km from the Archives, chosen as it is the closest WMO-compliant (World Meteorological Organisation) meteorological station. The 1.5 km distance from the Archives was assumed to have a negligible effect on local weather data. The weather station has been in operation since December 2012 (http://www.astropa.inaf.it/ (accessed on 15 January 2023)), and it is composed of a Campbell Scientific CR1000 data logger equipped with TTU 600 Hygroclip HC2 S3 ($\pm 0.8\%$ for RH, $\pm 0.1\,^{\circ}C$ for T, at 23 °C $\pm$ 5 °C), distributed by Rotronic® (Bassersdorf, Switzerland).

Before data mining, T and RH data were checked in terms of missing values through the completeness index (CoI) and the continuity index (CI) [36]. In addition, outdoor T observations registered in Palermo in the monitored period were compared with the IPCC past scenario (described in Section 2.2.1) to identify anomalies with respect to the climatological features of the IPCC dataset. To this purpose, climatological temperatures of each day of the year were computed over the period 1981–2010 (Recent Past, RP) with the 30-year medians of the i-th day of the year and smoothed out by the 30–days moving average centred on the i-th day under investigation. Then, the same procedure was applied to compute the 5th and 95th percentiles representing the climatological band.

2.2. Climate-Induced Risk Assessment

Within the context of risk management [2], the present investigation deals with the assessment of the risks related to incorrect T and RH and the presence of pests, focusing on the cumulative biodeterioration processes induced by the climate conditions at the building scale. To establish a link between the outdoor climate and deterioration processes, a three-level step approach (described in detail in the next subsections) is followed to assess climate-induced risks due to biodeteriogens. Starting from outdoor climate scenarios, the indoor ones were reconstructed through the application of heat transfer functions (TF). Then, projections of indoor and outdoor climate conditions are the input of dose–response functions useful to determine the climate-induced risk posed by biodeteriogens.

2.2.1. Climate Scenarios at the Mediterranean Site

The IPCC Sixth Assessment Report (AR6) has described multiple Shared Socioeconomic Pathways (SSPs) associated with different future emission scenarios (i.e., Representative Concentration Pathways, RCPs) [37]. Each SSP provides one possible scenario that would be brought along by possible socioeconomic conditions, land-use changes, and other human-caused climate drivers that influence greenhouse gas (GHG) emissions, thus affecting also the specific radiative forcing characteristics (i.e., the change in the net radiative flux).

Daily data of air T, mixing ratio (MR), and total precipitation (pr) related to the area of Palermo were extracted from the Copernicus Climate Data Store (CDS). The sixth phase's dataset of the *Coupled Model Intercomparison Project* (CMIP6) was chosen for both the Recent-Past climate (RP, 1981–2010) and the intermediate SSP scenarios for the Near-Future (NF, 2021–2050) and Far-Future (FF, 2071–2100) climates [38]. The CMIP6 dataset used in this analysis ($0.9° \times 1.25°$ grid resolution) was produced by the *Centro Euro-Mediterraneo sui Cambiamenti Climatici* (CMCC) [39], providing past atmospheric data from 1850 onward and future climate scenarios SSP1-2.6, SSP2-4.5, and SSP5-8.5. The IPCC-AR6 projections account for the following forcings:

- SSP1-2.6 represents a sustainable SSP where consumption and population growth are low, and the resulting GHG emissions correspond to a radiative forcing peak of 2.6 W·m^{-2} by 2100;
- SSP2-4.5 is an intermediate SSP representing a fossil-fuel-intensive world with a development pattern similar to the current one, in which the radiative forcing is stabilized at approximately 4.5 W·m^{-2} after 2100;
- SSP5-8.5 is a SSP representing a fossil-fuel-intensive world with the highest GHG emissions for which the radiative forcing reaches 8.5 W·m^{-2} by 2100.

Under the above scenarios, global warming of 1.5 °C above the pre-industrial levels is very likely to be exceeded before 2040 under SSP5-8.5, likely to be exceeded under SSP2-4.5, and more likely than not to be exceeded under SSP1-2.6 [37].

Outdoor T and MR data corresponding to the area of Palermo were used to derive indoor T and MR in the Recent-Past (RP, 1981–2010), Near-Future (NF, 2021–2040), and Far-Future (FF, 2071–2100) climates for the above SSP scenarios.

2.2.2. Indoor Climate Scenarios

A conduction heat transfer function was used to express the annual seasonal cycles of the indoor T and MR from the outdoor forcing factor [9,29,40]. Outdoor and indoor T and MR observations over a year were used to model the indoor and outdoor heat and moisture fluxes. The annual cycles were fitted as a generic time-dependent sinusoidal equation (Equation (1)):

$$x = \overline{x} + \Delta x \cdot \sin(\omega t - \varphi) \tag{1}$$

where x is the outdoor/indoor T or MR observation, t is time, $\overline{x}$ is the annual average of outdoor/indoor T or MR, ω is the angular frequency (i.e., $\omega = 2\pi/P$ where P is the period), Δx is the amplitude of T or MR (i.e., half of the maximum seasonal spread between minimum and maximum values over a year), and φ is the phase shift of the best-fit sine function. The indoor versus outdoor of both T and MR sinusoids can then be combined to obtain the annual hysteresis cycles describing the thermal and moisture inertia of the building envelope. In this case, an ellipse interpolates the points whose coordinates are the monthly averages of outdoor and indoor T or MR. The coordinates of the extreme points of the major axis of the ellipse are determined by the outdoor T or MR maximum seasonal spread, the ordinates of the extremes of the minor axis by the indoor T or MR variability. The tangent of the angle that the major axis of the ellipse forms with the abscissa is the ratio between the indoor and the outdoor ranges.

Once the sinusoidal equations were determined, starting from the outdoor T and MR scenarios, the T and MR cycles inside the Archives could be inversely simulated using the

sinusoidal equations. Assuming that the building envelope features negligibly change over time, a heat transfer function was set to reconstruct future indoor climate from the outdoor climate. RH values were computed from T and MR by using the formula in [35], without considering the moisture buffering effect of internal hygroscopic materials. In this way, it is possible to estimate the indoor climate in terms of T and RH associated with past and future outdoor scenarios as well as the evolution of biodeterioration risks in the Archives.

2.2.3. Biologically Related Dose–Response Functions

Specific dose–response functions (DRFs) were selected to quantify the occurrences of climate conditions favouring biodeteriogens usually proliferating in libraries and archives. Table 1 summarises the relationship between biodeteriogens and heritage materials (e.g., stone, cellulose-based material, and wood) together with the related DRFs. The most suitable DRFs to be used for quantifying the biodeterioration risk can be chosen based on the heritage materials that may be exposed to the presence of specific biodeteriogens as well as on the availability of the climate data required for the DRF calculation (Table 1).

Table 1. Summary of dose–response functions (DRFs) to assess favourable climate conditions for biodeteriogens (insects and moulds). Climate data collected over at least one whole year (or multiple): T = temperature, RH = relative humidity, pr = precipitation.

Materials		Biodeteriogens	Climate Variables	DRF	Ref.
Building stone	in	*Aspergillus fumigatus, Aspergillus flavus, Stachybotrys chartarum*	T, RH	Sedlbauer isopleths	[41]
	out	*Biofilm*	T, pr	Biomass accumulation	[42]
Cellulose-based		*Stegobium paniceum* (Linnaeus) (drugstore beetle)	T, RH	Development time (t_D)	[11]
			T	Growing degree days (GDDs)	
			T	Number of growth cycles for a year (N_{GC}) [*]	
		Tineola bisselliella (Hummel) (webbing clothes moths)	T	Eggs laid (E)	
Wood		*Anobium punctatum* (De Geer) (woodworm or furniture beetle) [**]	T	Flying degree days (FDDs)	[11,43]
			T	Growing degree days (GDDs)	[11]
		Alternaria alternata, Aspergillus species, Aureobasidium pullulans, Cladosporium cladosporioides, Chaetomium globosum, Paecilomyces variotii, Penicillium spp., *Trichoderma viride*	T, RH	VTT model	[41,44]

[*] Temperature-dependent adult male insects; [**] humidity-dependent adult male insects.

Several colonizers (bacteria, cyanobacteria, dematiaceous fungi, algae, lichens, mosses, etc.) can develop biofilms on outdoor rock surfaces. The final equilibrium state of the microbial composition of biofilm, namely biomass, depends on the climatic conditions, the nature of the substrate, and the exposure [42]. The outdoor biomass accumulation (B, mg·cm^{-2}) was estimated using Equation (2):

$$B = exp(-0.964 + 0.003 \cdot pr - 0.01 \cdot T) \tag{2}$$

where pr is the annual amount of precipitation (mm), and T is the annual mean temperature (°C).

The spores of mesophilic fungi, which are ubiquitous, become a biological risk when T > 20 °C and RH > 65% for a prolonged time [15,45]. The risk of mould fungi growth was assessed by comparing monthly T and RH scenarios with the Sedlbauer isopleths and the VTT model [41]. Sedlbauer isopleths are curves of equal risk describing the times

for spore germination and mycelial growth on four substrate categories. The critical RH (RH*) is associated with the lowest isopleth for mould (LIM), i.e., the lowest curve where mould activity is assumed to begin, for a specific substrate, thus assuming the worst conditions [41]. Equations (3) and (4) refer to spore germination (RH*$_{GERM}$) and mycelial growth (RH*$_{GROWTH}$), respectively, on biologically recyclable building materials (i.e., substrate category I):

$$RH^*_{GERM} = -1.5 \cdot 10^{-3} \cdot T^3 + 1.1 \cdot 10^{-1} \cdot T^2 - 2.6 \cdot T + 97 \tag{3}$$

$$RH^*_{GROWTH} = -1.4 \cdot 10^{-3} \cdot T^3 + 9.4 \cdot 10^{-2} \cdot T^2 - 2.2 \cdot T + 95 \tag{4}$$

where T is the air temperature (°C), and this equation is applied when T is <35 °C.

The VTT model relies on a standard mould index (M) based on the visual mould appearance of the surface under the study. The critical RH (RH*) can be expressed through Equation (5) for different T conditions [41,44]:

$$RH^*_{VTT} = -2.7 \cdot 10^{-3} \cdot T^3 + 1.6 \cdot 10^{-1} \cdot T^2 - 3.1 \cdot T + 100 \tag{5}$$

when T $\leq$ 20 °C, otherwise RH*$_{VTT}$ = 80%.

As for paper-based, textile, and wooden materials, insects are responsible for various damage, e.g., holes and tunnels excavated by larvae, consumption of adhesives and coatings, and wear and loss. Insect growth and development are mainly related to temperature (i.e., in warm conditions insects proliferate rapidly) and relative humidity (e.g., eggs and young larvae are sensitive to dehydration) [11]. However, the risk of insect infestation—which can be also favoured by the chemicophysical nature of the substrate, insufficient ventilation and inadequate lighting, together with the shortage of dusting/cleaning strategies and periodic handling—is relatively less studied in terms of usable dose–response functions. In general, insects need mild (i.e., T between 15 and 30 °C) and wetter (i.e., RH between 50% and saturation) environments that favour eggs, larvae, and mature insects' proliferation. On the contrary, when T and/or RH levels are low, some insects enter a comatose status for cold and/or dehydration. The threat of insect pest infestation was evaluated through three indices: (i) the number of eggs laid (E) by adult female webbing cloth moths (*Tineola bisselliella*), (ii) the number of growth cycles per year (N$_{GC}$) for temperature-dependent and humidity-dependent adult male insects (woodworm—*Anobium punctatum*), and (iii) the development time (t) for temperature-dependent adult male insects (drugstore beetle—*Stegobium paniceum*).

The number of eggs laid (E, expressed as an integer) by webbing cloth moths (*Tineola bisselliella*) can be computed according to Equation (6) [11]:

$$E = 130 \cdot exp\left(-\left(\frac{\frac{T^2-30}{30}}{12}\right)^2\right) \tag{6}$$

where T is the monthly temperature (°C). It is worth noting that, by its experimental definition, the maximum number of E per month is 130.

The number of growth cycles per year can be estimated by using growing degree days (GDDs) that are a measure of heat accumulation needed for the growth and development of plants and insects [43]. The growing degree days (GDDs) were defined as the sum (Σ) of the degrees that exceed reference T and RH every month (Equation (7)):

$$GDD = \sum_{D=1}^{365} \left(T_D - T_{ref}\right) \tag{7}$$

where T$_{ref}$ = 15 °C, T$_D$ is daily average temperature (°C) over the considered period, when RH > 30% for temperature-dependent and RH > 70% for humidity-dependent adult male insects.

The GDD values can be used to compute the number of growth cycles per year (N_{GC}, years^{-1}) for temperature-dependent male insects according to Equation (8):

$$N_{GC} = 0.0015 \cdot GDD + 0.272 \tag{8}$$

The development time (t_D, days) allows estimating the time it would take for both temperature-dependent (such as *S. paniceum*) and humidity-dependent adult male insects to develop in any given year (Equation (9)):

$$t_D = a + b \cdot T + c \cdot RH + d \cdot T^2 + f \cdot RH^2 + g \cdot T^3 + h \cdot RH^3 + i \cdot T \cdot RH + j \cdot T^2 \cdot RH + h \cdot T \cdot RH^2 \tag{9}$$

where a–k are constants obtained from a weighted least squares fit to a cubic polynomial surface, and their values are available in [11]. It is worth noticing that t_D is not allowed to be shorter than 40 days. Results can be displayed as isochrones (i.e., curves of equal t_D from paired T and RH).

3. Results

3.1. Characterisation of Current Climate Conditions

The time series of indoor T and RH collected over the period from 1 May 2021 to 30 April 2022, was found to be complete (CoI = 1, i.e., without missing data) and continuous (CI = 1, i.e., without intervals of missing data).

The comparison between the 30-year reference dataset (Recent Past, RP) and the outdoor T values measured in 2021 and 2022 at the *Osservatorio Astronomico di Palermo* identified anomalous cold and warm occurrences at the site under investigation. Figure 2 shows that about 25% of the daily outdoor T values exceed the upper threshold of the RP climatological band (above the 95th percentile), highlighting warmer conditions than those in the past. Only very few occurrences (4%) were colder than in 2021 (below the 5th percentile).
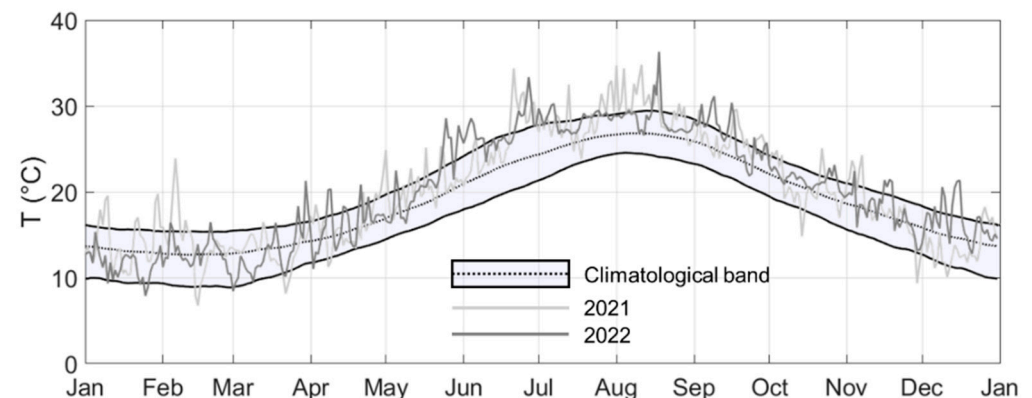

Figure 2. Daily outdoor temperatures in 2021 (light grey) and 2022 (dark grey) and the climatological band (coloured area) delimited by the 5th and 95th percentiles together with the climatological median values of the 30-year temperature data in RP (1981–2010).

Looking at Figure 3a, it can be noted that the box-and-whisker plots of the outdoor (out) and indoor (in) temperatures overlap, meaning that no significant difference is visible. Indeed, the T medians are 18.6 °C for outdoors and 20.0 °C for indoors with an interquartile range (IQR, i.e., difference between the 75th and 25th percentiles) of 11.3 °C and 10.3 °C, respectively. The smaller seasonal and daily variability in indoor T is evident in Figure 3b: T annual spread (i.e., $T_{max} - T_{min}$) is 16.9 °C with respect to 35.5 °C outdoors, whereas the range of T daily spans (i.e., daily $T_{max} - T_{min}$) is 0.1–1.8 °C with respect to 1.5–13.7 °C outdoors. The use of sinusoidal curves of the indoor and outdoor T data, estimating the seasonal cycles, allowed us to investigate the thermal inertia of the building envelope. From

Equation (1), the phase shift (φ) between the two cycles was calculated corresponding to a time of about 22 days. Figure 3c shows the scatter plot of the measured indoor versus outdoor hourly T (indicated as grey dots) and the ellipse resulting from the combination of indoor/outdoor sinusoidal curves and representing the seasonal thermal cycle inside the building (indicated as a red solid line). The ellipse centre corresponds to the annual arithmetic mean of the time series (T_{out} = 19.4 °C and T_{in} = 20.6 °C), whereas major and minor semi-axes are proportional to the outdoor and indoor T variability, respectively, and are equal to 11.1 °C and 1.5 °C.
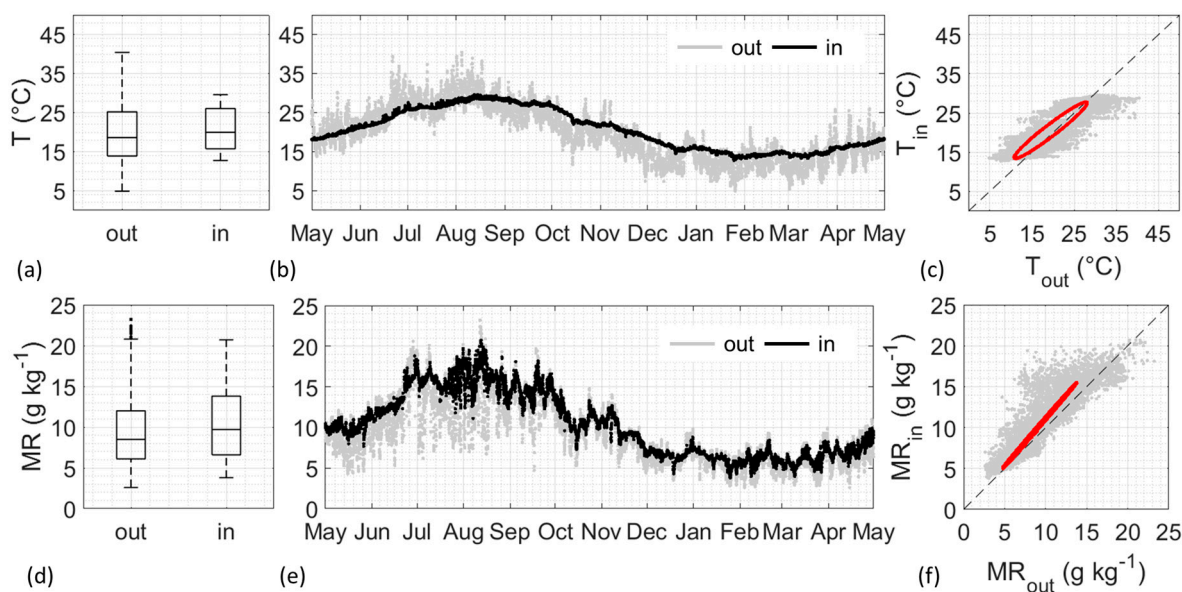

Figure 3. (**a**,**d**) Box-and-whisker plots of outdoor (out) and indoor (in) temperature (T) and mixing ratio (MR); (**b**,**e**) time plots of indoor (black) and outdoor (grey) T and MR; (**c**,**f**) indoor versus outdoor T and MR (grey dots) and the ellipse (red solid line) describing the annual hysteresis cycle in the Archives. In the box-and-whisker plots, the horizontal lines dividing each box indicate the medians.

The RH box-and-whisker plots (Figure 4a) overlap, showing no significant difference between indoor and outdoor observations. Indeed, RH medians are significantly coincident (RH_{median} = 64.0% with an IQR of 19.4% outdoor and 11.4% indoor). The smaller seasonal and daily variability in indoor RH is evident in Figure 4b: RH annual spread (i.e., RH_{max} − RH_{min}) is 44.8% with respect to 83.4% outdoors, whereas the range of RH daily spans (i.e., daily RH_{max} − RH_{min}) is 0.8–26.8% with respect to 8.1–63.5% outdoors. For RH, the ellipse was not applied, as RH is not a conservative variable. The indoor RH values for past and future conditions were computed from indoor T and MR.
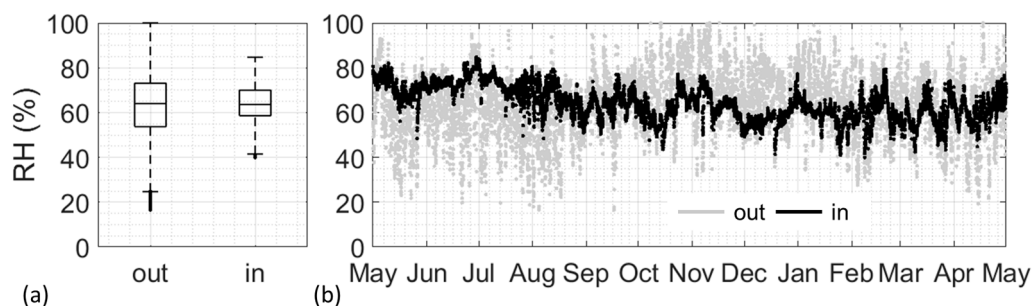

Figure 4. (**a**) Box-and-whisker plots of outdoor (out) and indoor (in) relative humidity; (**b**) time plots of indoor (black) and outdoor (grey) RH. In the box-and-whisker plots, the horizontal lines dividing each box indicate the medians, the black dots represent the outliers, s, i.e., the values above or below 1.5 × IQR (IQR = interquartile range).

3.2. Reconstruction of Indoor Climate Scenarios

Figure 5 shows the box-and-whisker plots of indoor T, MR, and RH in scenarios SSP1-2.6 (orange), SSP2-4.5 (blue), and SSP5-8.5 (green) for the Recent-Past (RP, 1981–2010), Near-Future (NF, 2021–2050), and Far-Future (FF, 2071–2100) climates. Both T and MR tend to increase from RP to NF and FF; whereas RH tends to decrease. The T, MR, and RH scenarios are significantly similar in NF (Table 2). On the contrary, the T–MR–RH conditions related to the three SSPs in the Far Future tend to be different moving from T_{median} = 22.5 °C for SSP2-2.6 to 24.6 °C for SSP5-8.5, from MR_{median} = 12.5 g·kg^{-1} for SSP1-2.6 to 14.0 g·kg^{-1} for SSP5-8.5 and from RH_{median} = 69.5% for SSP1-2.6 to 68.3% for SSP5-8.5 (Table 2).
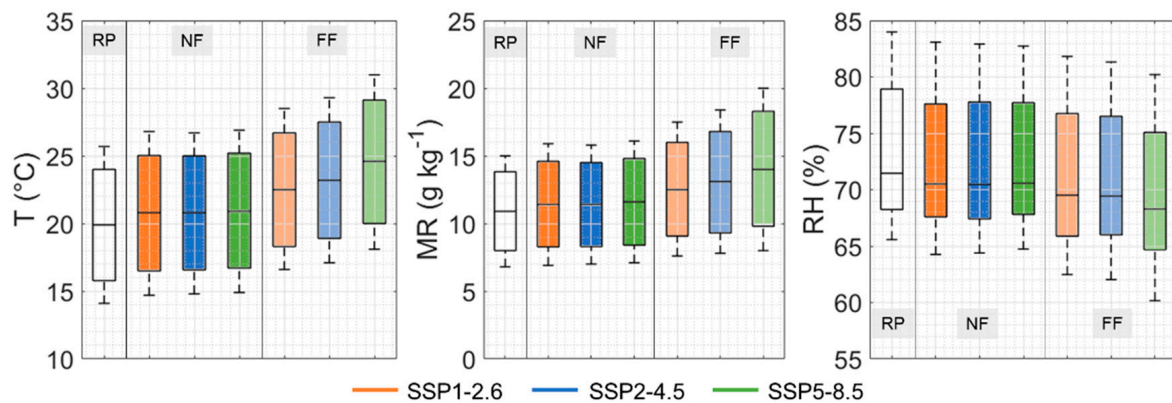

Figure 5. Box-and-whisker plots of indoor temperature (T), mixing ratio (MR), and relative humidity (RH) in scenarios SSP1-2.6 (orange), SSP2-4.5 (blue), and SSP5-8.5 (green) from Recent Past (RP, 1981–2010) to Near Future (NF, 2021–2050) and Far Future (FF, 2071–2100). In the box-and-whisker plots, the horizontal lines dividing each box indicate the medians.

Table 2. Summary of the statistical parameters for indoor temperature (T, °C) and mixing ratio (MR, g·kg^{-1}) data in scenarios SSP1-2.6 (orange), SSP2-4.5 (blue), and SSP5-8.5 (green) from Recent Past (RP, 1981–2010) to Near Future (NF, 2021–2050) and Far Future (FF, 2071–2100). (Q2 = median; IQR = interquartile range; Δy = maximum annual difference).

Climate Variable	Statistical Parameter	RP	NF			FF		
			SSP1-2.6	SSP2-4.5	SSP5-8.5	SSP1-2.6	SSP2-4.5	SSP5-8.5
T (°C)	Q2	19.9	20.8	20.8	20.9	22.5	23.2	24.6
	IQR	8.2	8.5	8.4	8.5	8.4	8.6	9.1
	Δy	11.6	12.1	11.9	12.0	11.9	12.2	12.9
MR (g·kg^{-1})	Q2	10.9	11.4	11.4	11.6	12.5	13.1	14.0
	IQR	5.8	6.3	6.2	6.4	6.9	7.5	8.5
	Δy	8.2	9.0	8.8	9.0	9.9	10.6	12.0
RH (%)	Q2	71.5	70.5	70.5	70.6	69.5	69.4	68.3
	IQR	10.7	10.0	10.4	9.9	10.9	10.5	10.4
	Δy	18.4	18.8	18.5	18.0	19.4	19.3	20.1

3.3. Risk of Biodeteriogens' Proliferation

The biomass accumulation (B, mg·cm^{-2}) was estimated from outdoor temperature (T) and precipitation (pr) scenarios using Equation (2). As the annual amount of pr tends to slightly decrease from RP (pr_{RP} = 476 mm) towards NF and FF ($pr_{SSP5-8.5}$ = 334 mm), and the annual mean temperature (T) tends to increase from RP (T_{RP} = 18.8 °C) towards NF and FF ($T_{SSP5-8.5}$ = 23.2 °C), the B values move from 1.3 mg·cm^{-2} in RP to a minimum of 0.8 mg·cm^{-2} in FF of SSP5-8.5.

Figure 6 shows the risk of mould colonisation inside the Archives. Each panel shows the lowest isopleth for mould (LIM) for spore germination (RH*$_{GERM}$, solid black line) and mycelial growth (RH*$_{GR}$, dashed black line), under which mould activity ceases for biologically recyclable building materials and wood (critical RH identified through the VTT model (RH*$_{VTT}$, dotted black line)). Grey asterisks show that the actual indoor climate conditions do not favour mould colonisation, as they are always under the critical RH* curves, thus explaining the absence of active moulds as documented in the survey conducted in 2018. The indoor climate conditions simulated in RP (black dots) are associated with a higher risk of mould colonisation compared to the indoor climate conditions resulting from the NF and FF climates under the three different SSPs. In all SSPs, there is a visible trend from RP to FF, particularly in the case of SSP5-8.5 (Figure 6c, light green dots), in which the indoor climate conditions tend to be less favourable for mould colonisation.
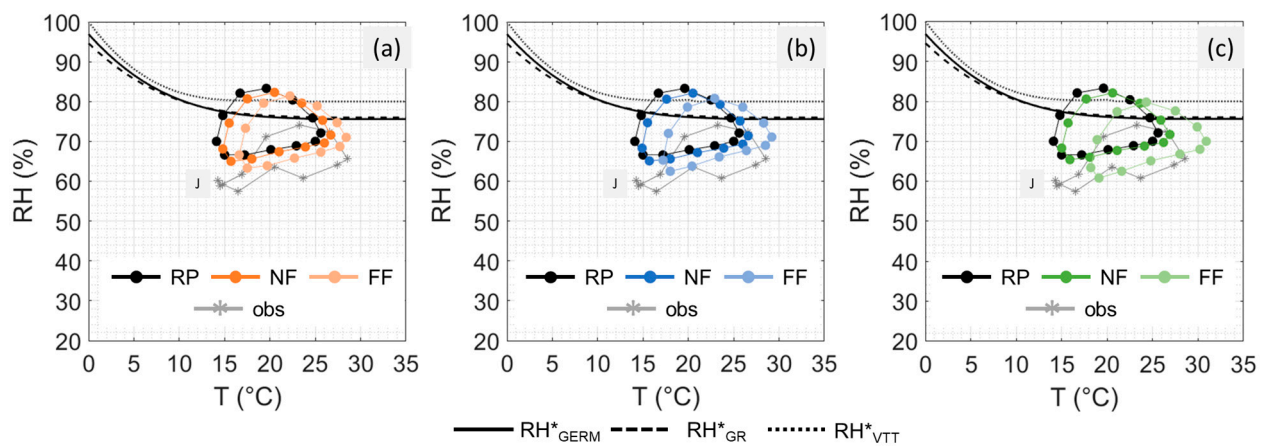

Figure 6. Monthly temperature (T) and relative humidity (RH) plotted together with the lowest isopleths for spore germination (solid lines, Equation (3)), mycelial growth (dashed lines, Equation (4)) according to Sedlbauer isopleths and the critical RH* (dotted lines, Equation (5)) according to the VTT model in measured conditions and scenarios SSP1-2.6 (**a**), SSP2-4.5 (**b**), and SSP5-8.5 (**c**) from Recent Past (RP, 1981–2010) to Near Future (NF, 2021–2050) and Far Future (FF, 2071–2100). Letter "J" in scatter plots indicates January with a clockwise direction of the annual cycle.

Figure 7 shows the indoor climate conditions favourable for the proliferation of adult insects responsible for degradation in archival materials. The number of eggs (E, Equation (6)) laid by the webbing cloth moth—*T. bisselliella*—(Figure 7a) slightly exceeds 450 units in current indoor climate conditions following the value expected in NF and increasing with respect to RP; in FF, the risk associated with the emission scenario SSP5-8.5 is almost three times higher than the value in RP (360 eggs). A similar trend resulted from the calculation of the growing degree days (GDDs) for temperature-dependent adult male individuals of drugstore beetle (*S. paniceum*), where the GDDs in current conditions are about 2090 units. Compared to RP, where GDDs were equal to 1800 units, the value increased in NF to 2100 units and up to 3500 units in FF under SSP5-8.5 (Figure 7b). It can be noticed that in both cases, the increase in the risk of insect pest infestation drastically worsens in the highest GHG emission scenario SSP5-8.5 (GDDs~3500 units) if compared to SSP1-2.6 and SSP2-4.5 (GDDs $\leq$ 3000 units). From these outcomes, the number of growth cycle per year were calculated according to Equation (8), showing that N$_{GC}$ value moves from 3 years^{-1} in RP up to N$_{GC}$ = 6 years^{-1} in FF SSP5-8.5. In the case of humidity-dependent adult male individuals of woodworm (*A. punctatum*), although GDDs in current conditions slightly exceed 650 due to low monthly RH values, GDDs show a positive trend from 1200 in RP to 1600 units, meaning that the decrease in humidity might represent a limitation for such biodeteriogens (Figure 7b). Figure 7c–e show the annual development time for a temperature-dependent adult male insect in the measured indoor climate conditions and in simulated scenarios SSP1-2.6, SSP2-4.5, and SSP5-8.5. In all circumstances, monthly T and

RH conditions lie in the risky area (outlined by dashed lines). It is clear that in scenario FF SSP5-8.5 (Figure 7e, light green dots), climate conditions favourable for insects' growth can occur over the whole year, and t never exceeds 150 days.
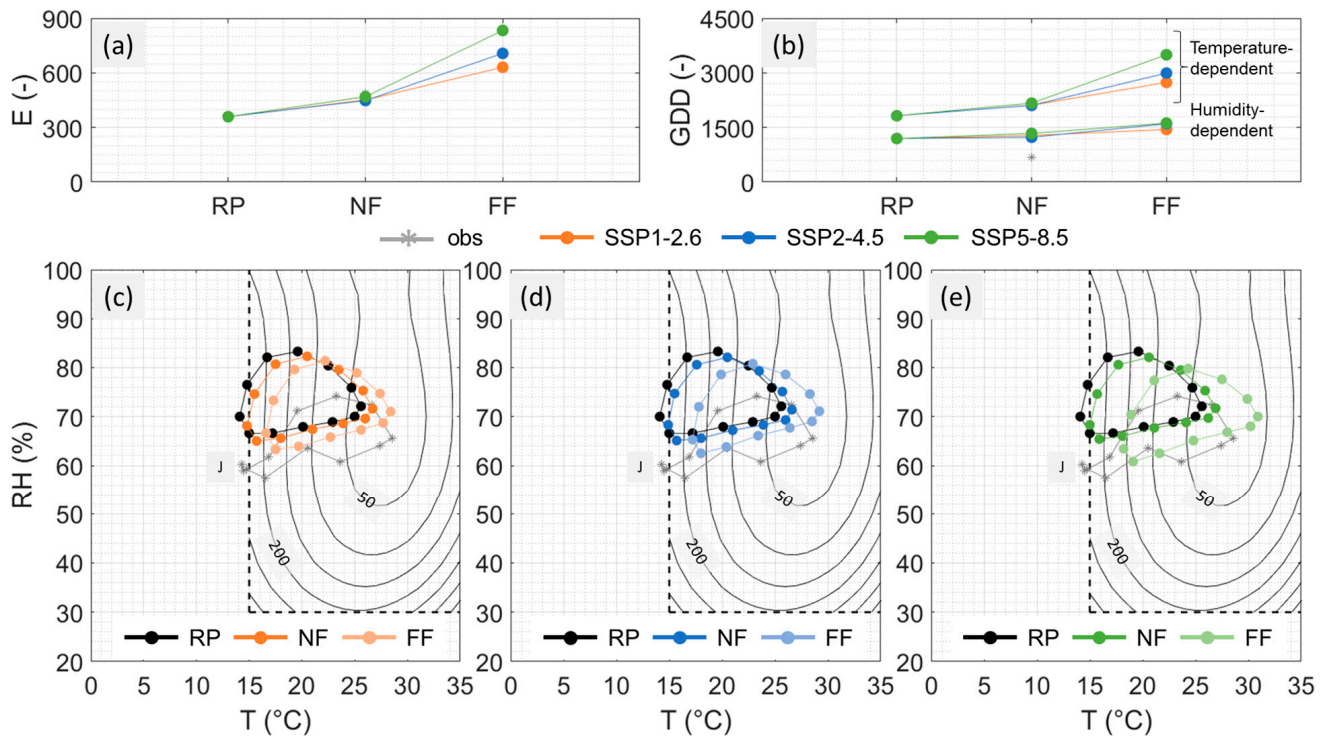

Figure 7. (**a**) Number of eggs laid (Equation (6)) over a representative year by webbing cloth moths (*T. bisselliella*) and (**b**) annual growing degree days (GDDs) for temperature-dependent (*S. paniceum*) and humidity-dependent (*A. punctatum*) adult male individuals (Equation (7)) from measured conditions, Recent-Past (RP, 1981–2010) to Near-Future (NF, 2021-2050) and Far-Future (FF, 2071–2100) climates under scenarios SSP1-2.6 (orange), SSP2-4.5 (blue), and SSP5-8.5 (green). (**c–e**) Monthly temperature and relative humidity conditions (coloured dots) plotted on development time curves (t_D, Equation (9)) indicating the time in days it would take for drugstore beetle (*S. paniceum*) to develop in a given year representative of measured conditions and scenarios SSP1-2.6, SSP2-4.5, and SSP5-8.5. Letter "J" in scatter plots indicates January with a clockwise direction of the annual cycle.

4. Discussion

4.1. Characterisation of Current Climate Conditions

The indoor climate conditions in the State Archives of Palermo (Figures 2 and 3) were compared with those reported in other Italian archives and libraries housed in unconditioned historical buildings: *Archive of the University Library* of Bologna [46], *Ca' Granda* (Milan) [6], *Classense* (Ravenna) [47], *Delfiniana* (Udine) [6], *Doctorate Library of the University of Perugia* [48], *Malatestiana* (Cesena) [49], and *Palatina* (Parma) [50]. In all these historical libraries including this case study investigated in this paper, the maximum annual indoor temperature exceeded 25 °C, beyond the safe threshold for chemical stability indicated in the standard [45]. Since the expected outdoor temperature increase will likely cause an increase in the indoor T, it becomes important to plan and implement right now adequate adaptation strategies to mitigate the risk of temperature-dependent deterioration and overheating in summertime [51]. In terms of the indoor relative humidity variations, the annual RH excursion experienced in Palermo is high compared to the RH stability (ΔRH = 10%) occurring in the *Archive of the University Library* of Bologna and *Palatina* (Parma) but similar in magnitude (i.e., ΔRH = 35%) to the one reported in *Ca' Granda* and *Malatestiana*. Even though it is not the aim of this research, the tendency of outdoor temperatures towards warmer conditions (Figure 2) may be interpreted as a warning signal that needs to be

considered, since it could be associated with modifications in biodeteriogens proliferation, and, generally speaking, in changes in materials' response.

4.2. Reconstruction of Indoor Climate Scenarios

The inverse modelling was reasonably applied to this case study as the building was not equipped with system for climate control, and hence, the indoor climate was predominantly influenced by the outdoor climate [29]. It was found that the phase shift between outdoor and indoor seasonal cycles corresponded to a time of about 22 days for T and 3 days for MR, meaning that the building acts as a good buffer against the outdoor short-term fluctuations of T but not for those of MR. This result was in accordance with that of Bertolin et al. [9], who applied the same approach to a small 15th-century gothic church embedded in the monastery complex of S. Giustina (Padua, Italy). Indeed, the vapour exchanges may be governed by air convection through the openings (i.e., low moisture buffering [52]), while the thermal effect may be attenuated by the higher heat capacity of the walls compared to the circulating air.

The main advantage of inverse modelling approach against the use of whole building dynamic simulation is the capability of simulating the seasonal evolution of temperature and humidity in buildings without hygrothermal gains not driven by outdoor conditions. On the contrary, if a detailed characterisation of hygrothermal performance of the building is required along with a higher time resolution, the inverse modelling approach based on the transfer functions cannot be applied. In this case, the whole-building dynamic simulation hygrothermal modelling is necessary [53] but requires high expertise as well as detailed information on the building that is often inaccessible in the case of historical buildings [8,54,55]. Therefore, further application of the inverse modelling approach can be encouraged to study the seasonal evolution of the indoor climate in unconditioned heavyweight historical buildings also in other compatible sites in the Mediterranean area.

Finally, notwithstanding the modelling approach followed, it is fundamental to be aware that local weather data are highly recommended for characterising the outdoor climate surrounding the building. Nevertheless, the outdoor Global Climate Model, having a coarse spatial resolution, might not be able to accurately estimate the conditions at the district/building level. Advanced interpolation methods might be used to derive climate data at higher spatial resolution than the one currently available for CMIP6 data [16].

4.3. Risk of Biodeteriogens' Proliferation

The Sedlbauer isopleths and VTT model supported the assessment of biodeteriogens' risks, as they define climate conditions conducive to the proliferation of biodeteriogens that have been widely sampled also in other Italian libraries and archives housed in unconditioned historical buildings, such as *Alternaria* sp., *Aspergillus* sp., *Cladosporium* sp., *Penicillium* sp. (e.g., in the "*Doctorate Library*" of the University of Perugia [48], in the book depository at *Forte Belvedere* in Florence [56], and in the *Palatina* library in Parma [50]). In the case of the *State Archives* of Palermo, it was found that spore germination and mould growth were less favoured in the coming years thanks to lower relative humidity levels. However, as highlighted by Brimblecombe et al. [17], fungi might still be detected in the interior of closed cupboards due to high water content of materials that can favour enough mould's growth. It is also worth noticing that xerophilic moulds such as *Eurotium halophilicum* can grow also in drier conditions [57]. While the development of colonies of mesophilic fungi can lead to a severe loss of paper material, *E. halophilicum* is usually responsible for characteristic efflorescence on the backs and cuts of archival folders and/or in metal cabinets, display cases and safety accessories in rubber, etc. The expected persistence of warm conditions in the *State Archives* could favour temperature-dependent adult insects' proliferation up to three times as much as in the past and current conditions. Although the presence of living insects has not been reported in the survey, the damage signs on some books suggest that infestations occurred in the past. This evidence stresses the importance

of starting to plan right now strategies to limit the access of adult insects in the space, as their proliferation might be greatly favoured by the high future temperatures, particularly in the occurrence of scenario SSP5-8.5. As an example, vulnerable collections should not be placed in areas nearby windows to reduce the infestations by *S. paniceum* which is strongly attracted by light [17]. The assessment of the risk of both moulds and insects confirmed the results from [7,30].

5. Conclusions

The present study aimed at assessing the risk due to the proliferation of biodeteriogens likely present in a southern Mediterranean site under different IPCC climate scenarios. The State Archives of Palermo (Italy), housed in a 15th-century convent, were used for this case study. The main outcome of this paper is the definition of a practical and interdisciplinary approach that can effectively support the planning of preventive conservation strategies to limit the future biodeterioration of cultural heritage. First, a conduction heat transfer function is used to describe the relationship between the observed outdoor and indoor climates in unconditioned historical buildings. Then, this heat transfer function is applied to retrieve indoor climate from past and future outdoor climates. Finally, dose–response functions are used to assess the risk due to a wide range of biodeteriogens responsible for the deterioration of heritage materials (e.g., stone, cellulose-based material, and wood). Involving both biological and climate disciplines, the investigation allowed for a comprehensive assessment of the current and future biodeterioration risks.

The actual indoor climate in the Archives is characterised by a maximum annual indoor temperature exceeding 25 °C and high relative humidity variations compared to other historical libraries. The parameters fitting the heat and moisture transfer functions showed that the historical building acts as a good buffer throughout the year in terms of short-term fluctuations of temperature but responds quickly to outdoor changes in the air mixing ratio. The observed conditions do not favour the mould risk, explaining the absence of active colonies reported after a biological field survey conducted in 2018. Nevertheless, considering the future IPCC climate scenarios (where both the indoor temperature and the mixing ratio are expected to raise), the assessment of climate-induced risk highlighted an increased risk of temperature-dependent adult insects' proliferation (up to three times as much as in the past and current conditions), accompanied by a decreased risk of spore germination and mould growth. These results allow for the design of tailored preventive conservation measures to enhance the durability of both the archival collections and the building and may give useful insights for other unconditioned historical buildings located in Mediterranean countries and having similar local weather conditions to those of the State Archives of Palermo.

The inverse modelling approach has proved to be an effective alternative to a more complex and expertise-demanding whole-building dynamic simulation for PC studies aiming at assessing the global seasonal tendency in the climate-induced deterioration risks. However, since the inverse modelling involves smoothing out short-term indoor hygrothermal fluctuations, it cannot capture the peak conditions in the temperature (e.g., overheating in summertime) and humidity that may occur more frequently as a consequence of climate change. Moreover, due to the coarse spatial scale of the outdoor Global Climate Model, the obtained outputs may differ from the exact conditions at each point of the grid area and cannot accurately estimate the conditions at the district/building level. Future research will need to employ climate data at higher resolution or to interpolate climate data at a finer grid. In addition, the simulation of the indoor relative humidity can be further implemented, as it has not currently considered accurate moisture transfer models and the buffering effect of hygroscopic materials. Further application of the inverse modelling approach proposed in this paper is encouraged to create a database that collects the coefficients describing the response of unconditioned historical buildings and, hence, to study the seasonal evolution of the indoor climate in other comparable (similar) sites in the Mediterranean area.

References

1. ICOM-CC. *Terminology to Characterize the Conservation of Tangible Cultural Heritage*; ICOM-CC: Paris, France, 2008.
2. Pedersoli, J.L.J.; Antomarchi, C.; Michalski, S. *A Guide to Risk Management of Cultural Heritage*; ICCROM, CCI, Eds.; International Centre for the Study of the Preservation and Restoration of Cultural Property: Rome, Italy, 2016; ISBN 9789290772491.
3. Strlič, M.; Thickett, D.; Taylor, J.; Cassar, M. Damage Functions in Heritage Science. *Stud. Conserv.* **2013**, *58*, 80–87. [CrossRef]
4. Bonazza, A.; Sardella, A. Climate Change and Cultural Heritage: Methods and Approaches for Damage and Risk Assessment Addressed to a Practical Application. *Heritage* **2023**, *6*, 3578–3589. [CrossRef]
5. Sesana, E.; Gagnon, A.S.; Ciantelli, C.; Cassar, J.A.; Hughes, J.J. Climate Change Impacts on Cultural Heritage: A Literature Review. *Wiley Interdiscip. Rev. Clim. Chang.* **2021**, *12*, e710. [CrossRef]
6. Verticchio, E.; Frasca, F.; Bertolin, C.; Siani, A.M. Climate-Induced Risk for the Preservation of Paper Collections: Comparative Study among Three Historic Libraries in Italy. *Build. Environ.* **2021**, *206*, 108394. [CrossRef]
7. Leissner, J.; Kilian, R.; Kotova, L.; Jacob, D.; Mikolajewicz, U.; Broström, T.; Ashley-Smith, J.; Schellen, H.L.; Martens, M.; Van Schijndel, J.; et al. Climate for Culture: Assessing the Impact of Climate Change on the Future Indoor Climate in Historic Buildings Using Simulations. *Herit. Sci.* **2015**, *3*, 38. [CrossRef]
8. Frasca, F.; Verticchio, E.; Cornaro, C.; Siani, A.M. Performance Assessment of Hygrothermal Modelling for Diagnostics and Conservation in an Italian Historical Church. *Build. Environ.* **2021**, *193*, 107672. [CrossRef]
9. Bertolin, C.; Camuffo, D.; Bighignoli, I. Past Reconstruction and Future Forecast of Domains of Indoor Relative Humidity Fluctuations Calculated According to EN 15757. *Energy Build* **2015**, *102*, 197–206. [CrossRef]
10. Bučková, M.; Puškárová, A.; Sclocchi, M.C.; Bicchieri, M.; Colaizzi, P.; Pinzari, F.; Pangallo, D. Co-Occurrence of Bacteria and Fungi and Spatial Partitioning during Photographic Materials Biodeterioration. *Polym. Degrad. Stab.* **2014**, *108*, 1–11. [CrossRef]
11. Brimblecombe, P.; Lankester, P. Long-Term Changes in Climate and Insect Damage in Historic Houses. *Stud. Conserv.* **2013**, *58*, 13–22. [CrossRef]
12. *EN 16790*; Conservation of Cultural Heritage—Integrated Pest Management (IPM) for Protection of Cultural Heritage. European Committee for Standardization: Brussels, Belgium, 2016.
13. Querner, P.; Sterflinger, K.; Piombino-Mascali, D.; Morrow, J.J.; Pospischil, R.; Piñar, G. Insect Pests and Integrated Pest Management in the Capuchin Catacombs of Palermo, Italy. *Int. Biodeterior. Biodegrad.* **2018**, *131*, 107–114. [CrossRef]
14. Brimblecombe, P.; Querner, P. Webbing Clothes Moth Catch and the Management of Heritage Environments. *Int. Biodeterior. Biodegrad.* **2014**, *96*, 50–57. [CrossRef]
15. Chapter 24, Museums, Galleries, Archives, and Libraries. In *ASHRAE Handbook—HVAC Applications*; American Society of Heating Refrigerating and Air-Conditioning Engineers: Atlanta, GA, USA, 2019.
16. Kotova, L.; Leissner, J.; Winkler, M.; Kilian, R.; Bichlmair, S.; Antretter, F.; Moßgraber, J.; Reuter, J.; Hellmund, T.; Matheja, K.; et al. Making Use of Climate Information for Sustainable Preservation of Cultural Heritage: Applications to the KERES Project. *Herit. Sci.* **2023**, *11*, 18. [CrossRef]
17. Brimblecombe, P.; Sterflinger, K.; Derksen, K.; Haltrich, M.; Querner, P. Thermohygrometric Climate, Insects and Fungi in the Klosterneuburg Monastic Library. *Heritage* **2022**, *5*, 4228–4244. [CrossRef]
18. Lankester, P.; Brimblecombe, P. Future Thermohygrometric Climate within Historic Houses. *J. Cult. Herit.* **2012**, *13*, 1–6. [CrossRef]
19. ICOMOS. ICOMOS Statement to the United Nations Climate Change Conference (COP27) 2022. Available online: https://www.icomos.org/images/DOCUMENTS/Secretariat/2022/COP27/Statement_ICOMOS_COP27_20221106_EN.pdf (accessed on 1 February 2023).

20.　Climate Heritage Network. *Empowering People to Imagine and Realise Climate Resilient Futures Through Culture—From Arts to Heritage*; Climate Heritage Network: Wadi Musa, Jordan, 2022.

21.　IPCC. Assessment Report 6 Climate Change 2021: The Physical Science Basis. Available online: https://www.ipcc.ch/report/ar6/wg1/ (accessed on 15 January 2023).

22.　IPCC. *Climate Change 2023: Synthesis Report. A Report of the Intergovernmental Panel on Climate Change. Contribution of Working Groups I, II and III to the Sixth Assessment Report of the Intergovernmental Panel on Climate Change*; IPCC: Geneva, Switzerland, 2023.

23.　Bertolin, C. Preservation of Cultural Heritage and Resources Threatened by Climate Change. *Geosciences* **2019**, *9*, 250. [CrossRef]

24.　Lankester, P.; Brimblecombe, P. The Impact of Future Climate on Historic Interiors. *Sci. Total Environ.* **2012**, *417–418*, 248–254. [CrossRef] [PubMed]

25.　Querner, P.; Sterflinger, K.; Derksen, K.; Leissner, J.; Landsberger, B.; Hammer, A.; Brimblecombe, P. Climate Change and Its Effects on Indoor Pests (Insect and Fungi) in Museums. *Climate* **2022**, *10*, 103. [CrossRef]

26.　Toledo, F. *The Role of Architecture in Preventive Conservation*; International Centre for the Study of the Preservation and Restoration of Cultural Property: Rome, Italy, 2006; Volume 74.

27.　*EN 16883*; Conservation of Cultural Heritage-Guidelines for Improving the Energy Performance of Historic Buildings. European Committee for Standardization: Brussels, Belgium, 2017.

28.　Frasca, F.; Cornaro, C.; Siani, A.M. A Method Based on Environmental Monitoring and Building Dynamic Simulation to Assess Indoor Climate Control Strategies in the Preventive Conservation within Historical Buildings. *Sci. Technol. Built. Environ.* **2019**, *25*, 1253–1268. [CrossRef]

29.　Camuffo, D.; Bertolin, C.; Bonazzi, A.; Campana, F.; Merlo, C. Past, Present and Future Effects of Climate Change on a Wooden Inlay Bookcase Cabinet: A New Methodology Inspired by the Novel European Standard EN 15757. *J. Cult. Herit.* **2014**, *15*, 26–35. [CrossRef]

30.　Sabbioni, C.; Cassar, M.; Brimblecombe, P.; Tidblad, J.; Kozlowski, R.; Drdácký, M.; Ariño, X. Global Climate Change Impact on Built Heritage and Cultural Landscapes. In Proceedings of the International Conference on Heritage, Weathering and Conservation, HWC, Madrid, Spain, 21–24 June 2006; Gomez-Heras, Vazquez-Calvo, Eds.; Taylor & Francis Group: London, UK, 2006; pp. 395–401.

31.　Dias Pereira, L.; Saraiva, N.B.; Soares, N. Hygrothermal Behavior of Cultural Heritage Buildings and Climate Change: Status and Main Challenges. *Appl. Sci.* **2023**, *13*, 3445. [CrossRef]

32.　Beck, H.E.; Zimmermann, N.E.; McVicar, T.R.; Vergopolan, N.; Berg, A.; Wood, E.F. Present and Future Köppen-Geiger Climate Classification Maps at 1-Km Resolution. *Sci. Data* **2018**, *5*, 180214. [CrossRef] [PubMed]

33.　Gallo, A. *La Lotta Antitermitica in Italia—Commissione Interministeriale per La Lotta Antitermitica Roma*; Novagrafia: Roma, Italy, 1952.

34.　*EN 15758*; Conservation of Cultural Property—Procedures and Instruments for Measuring Temperatures of the Air and the Surfaces of Objects. European Committee for Standardization: Brussels, Belgium, 2010.

35.　*EN 16242*; Conservation of Cultural Heritage—Procedures and Instruments for Measuring Humidity in the Air and Moisture Exchanges between Air and Cultural Property. European Committee for Standardization: Brussels, Belgium, 2012.

36.　Frasca, F.; Siani, A.M.; Casale, G.R.; Pedone, M.; Bratasz, L.; Strojecki, M.; Mleczkowska, A. Assessment of Indoor Climate of Mogiła Abbey in Kraków (Poland) and the Application of the Analogues Method to Predict Microclimate Indoor Conditions. *Environ. Sci. Pollut. Res.* **2017**, *24*, 13895–13907. [CrossRef] [PubMed]

37.　Pörtner, H.O.; Roberts, D.C.; Adams, H.; Adelekan, I.; Adler, C.; Adrian, R. Technical Summary. In *Climate Change 2022: Impacts, Adaptation and Vulnerability. Contribution of Working Group II to the Sixth Assessment Report of the Intergovernmental Panel on Climate Change*; Pörtner, H.O., Roberts, D.C., Poloczanska, E.S., Mintenbeck, K., Tignor, M., Alegría, A., Craig, M., Langsdorf, S., Löschke, S., Möller, V., et al., Eds.; Cambridge University Press: Cambridge, UK; New York, NY, USA, 2022; pp. 37–118.

38.　O'Neill, B.C.; Tebaldi, C.; van Vuuren, D.P.; Eyring, V.; Friedlingstein, P.; Hurtt, G.; Knutti, R.; Kriegler, E.; Lamarque, J.-F.; Lowe, J.; et al. The Scenario Model Intercomparison Project (ScenarioMIP) for CMIP. *Geosci. Model Dev.* **2016**, *9*, 3461–3482. [CrossRef]

39.　Lovato, T.; Peano, D.; Butenschön, M.; Materia, S.; Iovino, D.; Scoccimarro, E.; Fogli, P.G.; Cherchi, A.; Bellucci, A.; Gualdi, S.; et al. CMIP6 Simulations with the CMCC Earth System Model (CMCC-ESM2). *J. Adv. Model Earth Syst.* **2022**, *14*, e2021MS002814. [CrossRef]

40.　Verticchio, E.; Frasca, F.; Garcìa-Diego, F.J.; Siani, A.M. Investigation on the Use of Passive Microclimate Frames in View of the Climate Change Scenario. *Climate* **2019**, *7*, 98. [CrossRef]

41.　Vereecken, E.; Roels, S. Review of Mould Prediction Models and Their Influence on Mould Risk Evaluation. *Build. Environ.* **2012**, *51*, 296–310. [CrossRef]

42.　Gómez-Bolea, A.; Llop, E.; Ariño, X.; Saiz-Jimenez, C.; Bonazza, A.; Messina, P.; Sabbioni, C. Mapping the Impact of Climate Change on Biomass Accumulation on Stone. *J. Cult. Herit.* **2012**, *13*, 254–258. [CrossRef]

43.　Camuffo, D.; Bertolin, C. Unfavorable Microclimate Conditions in Exhibition Rooms: Early Detection, Risk Identification, and Preventive Conservation Measures. *J. Paleontol. Tech.* **2016**, *15*, 144–161.

44.　Kuka, E.; Cirule, D.; Andersone, I.; Andersons, B.; Fridrihsone, V. Conditions Influencing Mould Growth for Effective Prevention of Wood Deterioration Indoors. *Appl. Sci.* **2022**, *12*, 975. [CrossRef]

45.　*EN 16893*; Conservation of Cultural Heritage—Specifications for Location, Construction and Modification of Buildings or Rooms Intended for the Storage or Use of Heritage Collections. European Committee for Standardization: Brussels, Belgium, 2018.

46. Boeri, A.; Longo, D.; Fabbri, K.; Pretelli, M.; Bonora, A.; Boulanger, S. Library Indoor Microclimate Monitoring with and without Heating System. *A Bologna University Library Case Study. J. Cult. Herit.* **2022**, *53*, 143–153. [CrossRef]

47. Andretta, M.; Coppola, F.; Seccia, L. Investigation on the Interaction between the Outdoor Environment and the Indoor Microclimate of a Historical Library. *J. Cult. Herit.* **2016**, *17*, 75–86. [CrossRef]

48. Ruga, L.; Bonofiglio, T.; Orlandi, F.; Romano, B.; Fornaciari, M. Analysis of the Potential Fungal Biodeteriogen Effects in the "Doctorate Library" of the University of Perugia, Italy. *Grana* **2008**, *47*, 60–69. [CrossRef]

49. Fabbri, K.; Pretelli, M. Heritage Buildings and Historic Microclimate without HVAC Technology: Malatestiana Library in Cesena, Italy, UNESCO Memory of the World. *Energy Build.* **2014**, *76*, 15–31. [CrossRef]

50. Pasquarella, C.; Balocco, C.; Saccani, E.; Capobianco, E.; Viani, I.; Veronesi, L.; Pavani, F.; Pasquariello, G.; Rotolo, V.; Palla, F.; et al. Biological and Microclimatic Monitoring for Conservation of Cultural Heritage: A Case Study at the De Rossi Room of the Palatina Library in Parma. *Aerobiologia* **2020**, *36*, 105–111. [CrossRef]

51. Verticchio, E.; Frasca, F.; Cavalieri, P.; Teodonio, L.; Fugaro, D.; Siani, A.M. Conservation Risks for Paper Collections Induced by the Microclimate in the Repository of the Alessandrina Library in Rome (Italy). *Herit. Sci.* **2022**, *10*, 80. [CrossRef]

52. Gagliano, A.; Nocera, F.; Patania, F.; Moschella, A.; Detommaso, M.; Evola, G. Synergic Effects of Thermal Mass and Natural Ventilation on the Thermal Behaviour of Traditional Massive Buildings. *Int. J. Sustain. Energy* **2016**, *35*, 411–428. [CrossRef]

53. Akkurt, G.G.; Aste, N.; Borderon, J.; Buda, A.; Calzolari, M.; Chung, D.; Costanzo, V.; Del Pero, C.; Evola, G.; Huerto-Cardenas, H.E.; et al. Dynamic Thermal and Hygrometric Simulation of Historical Buildings: Critical Factors and Possible Solutions. *Renew. Sustain. Energy Rev.* **2020**, *118*, 109509. [CrossRef]

54. Rajčić, V.; Skender, A.; Damjanović, D. An Innovative Methodology of Assessing the Climate Change Impact on Cultural Heritage. *Int. J. Archit. Herit.* **2018**, *12*, 21–35. [CrossRef]

55. Huerto-Cardenas, H.E.; Leonforte, F.; Aste, N.; Del Pero, C.; Evola, G.; Costanzo, V.; Lucchi, E. Validation of Dynamic Hygrothermal Simulation Models for Historical Buildings: State of the Art, Research Challenges and Recommendations. *Build. Environ.* **2020**, *180*, 107081. [CrossRef]

56. Menicucci, F.; Palagano, E.; Michelozzi, M.; Cencetti, G.; Raio, A.; Bacchi, A.; Mazzeo, P.P.; Cuzman, O.A.; Sidoti, A.; Guarino, S.; et al. Effects of Trapped-into-Solids Volatile Organic Compounds on Paper Biodeteriogens. *Int. Biodeterior. Biodegrad.* **2022**, *174*, 105469. [CrossRef]

57. Polo, A.; Cappitelli, F.; Villa, F.; Pinzari, F. Biological Invasion in the Indoor Environment: The Spread of Eurotium Halophilicum on Library Materials. *Int. Biodeterior. Biodegrad.* **2017**, *118*, 34–44. [CrossRef]